Vapor segregation and loss in basaltic melts

Marie Edmonds*
Hawaiian Volcano Observatory, U.S. Geological Survey, 51 Crater Rim Drive, Hawaii National Park, Hawaii 96718, USA
Terrence M. Gerlach
Cascades Volcano Observatory, U.S. Geological Survey, 1300 SE Cardinal Court #100, Vancouver, Washington 98683-9589, USA

ABSTRACT

Measurements of volcanic gases at Pu`u`Ō`ō, Kilauea Volcano, Hawai`i, reveal distinct degassing regimes with respect to vapor segregation and loss during effusive activity in 2004–2005. Three styles of vapor loss are distinguished by the chemical character of the emitted volcanic gases, measured by open path Fourier transform infrared spectroscopy: (1) persistent continuous gas emission, (2) gas piston events, and (3) lava spattering. Persistent continuous gas emission is associated with magma ascent and degassing beneath the crater vents, then eruption of the degassed magma from flank vents. Gas piston events are the result of static gas accumulation at depths of 400–900 m beneath Pu`u`Ō`ō. A CO_2-rich gas slug travels up the conduit at a few meters per second, displacing magma as it expands. Lava spattering occurs due to dynamic bubble coalescence in a column of relatively stagnant magma. The large gas bubbles are H_2O rich and are generated by open-system degassing at depths of <150 m. Static gas accumulation and dynamic bubble coalescence are both manifestations of vapor segregation in basaltic melts, but their implications differ. Accumulation and segregation of CO_2-rich vapor at depth does not deplete the melt of H_2O (required to drive lava fountains near to the surface) and therefore gas piston events can occur interspersed with lava fountaining activity. Lava spattering, however, efficiently strips H_2O-rich vapor from magma beneath the crater vents; the magma must then erupt effusively from vents on the flank of the cone.

Keywords: Hawai`i, Kilauea, magma degassing, vapor segregation, basalt, open path Fourier transform infrared spectroscopy.

INTRODUCTION

Basaltic magmas with dissolved volatiles may degas in a number of ways; this is one of the primary controls on the style of volcanic activity (Jaupart and Tait, 1990). At high rates of decompression bubbles expand quickly, resulting in rapid vesiculation, fragmentation, and explosive eruption (Head and Wilson, 1987). For low-viscosity magmas at low decompression rates, bubbles grow in dynamic equilibrium with the melt, gases segregate from the magma, and effusive eruption occurs. A mechanism for melt-gas segregation may be the rise of large bubbles through the melt, formed by the dynamic coalescence of smaller bubbles (Herd and Pinkerton, 1997) or the static coalescence of bubbles at the roof of a magma chamber (Jaupart and Vergniolle, 1989). Gas segregation processes in a volcanic conduit cannot be observed directly; however, the chemical composition of gas slugs and bubbles can be determined using remote spectroscopic techniques, allowing limits to be placed on the depth and style of gas segregation and a better understanding of how basaltic eruptions occur.

Magma ascends beneath the summit of Kilauea and is stored in a reservoir at 2.5–4.0 km (Ryan et al., 1981). CO_2-rich bubbles rise through the magma, accumulate, and escape through the chamber roof, giving rise to large CO_2 fluxes from Kilauea caldera (Gerlach et al., 2002). Magma migrates into the East Rift zone before ascending and erupting at Pu`u`Ō`ō (Fig. 1A). Lava erupted from established vents on the south flank of Pu`u`Ō`ō during 2004–2005. Much of the gas plume, however, emanated from vents inside the crater (Fig. 1A); this illustrates a large degree of vapor segregation from the melt. The gas plume mainly comprises water (H_2O) and sulfur dioxide (SO_2), which exsolve from the melt at depths of <100 m and, to a lesser extent, carbon dioxide (CO_2; Gerlach and Graeber, 1985). The gas composition can be measured accurately and remotely at Pu`u`Ō`ō using open path Fourier transform infrared spectroscopy (OP FTIR).

OP FTIR is a remote spectroscopic technique that utilizes the precise absorptivity of a particular gas. The method has proven useful for determining the concentration ratios of common volcanic gas species, such as H_2O, CO_2, SO_2, HCl, HF, and CO (e.g., Allard et al., 2005; Oppenheimer et al., 2006) at a high temporal resolution. In this paper we present data that illustrate the complexity and range of vapor-melt segregation processes during effusive basaltic eruptions. Volcanic gas compositions are only rarely quantified during dynamic eruptive activity; here the emitted gases were measured accurately and remotely, with a high degree of temporal resolution. Gases emitted during three distinct regimes were investigated: (1) persistent continuous degassing, (2) gas pistoning, and (3) lava spattering. Persistent continuous degassing is the typical degassing style at Pu`u`Ō`ō, characterized by emissions of a gas plume from crater vents and lava effusion from flank vents. Gas piston events were originally described by Swanson et al. (1979) during the Mauna Ulu eruption of 1969–1971: the top of a standing column of lava slowly rose from 30 to 50 m to the surface in 10–15 min. Lava spilled out, spattering began from the drowned fissure, and then the pooled lava rapidly drained back, accompanied by vigorous spattering and gas discharge. Gas piston events are relatively common at Pu`u`Ō`ō (Fig. 1B), although not always associated with synchronous eruption of lava. Lava spattering, which occurs independently of gas pistoning, is the ejection of gas and globs of lava from a vent to a height of few tens of meters (Fig. 1B), caused by the bursting of large, overpressurized bubbles at the top of a magma column (e.g., Tazieff, 1994).

METHOD AND RESULTS

Data were collected using a MIDAC Corporation infrared (IR) spectrometer, which consists of a Michelson interferometer, sterling-cooled indium antimonide (InSb) detector, and Newtonian telescope. Incandes-

*Current address: Earth Sciences Department, University of Cambridge, Downing Street, Cambridge CB2 3EQ, UK.

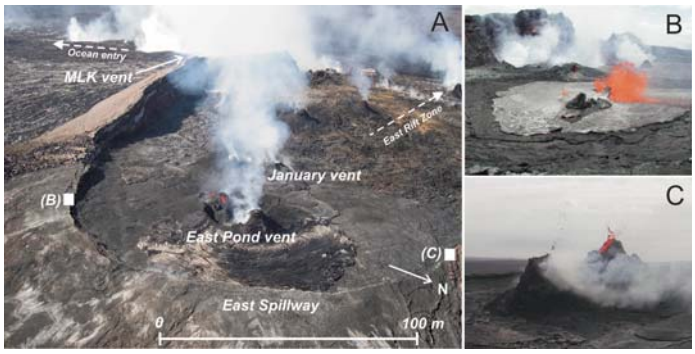

Figure 1. A: Oblique aerial photograph looking southwest showing crater vents at Pu`u`Ō`ō. Locations where measurements (*B*) and photos (*C*) were taken are labeled. B: Gas piston event. C: Lava spattering.

cent vents at a distance of <100 m were used as a source of IR radiation for the measurements; spectra were collected at a rate of 1 Hz and 8 spectra were added. Absorbance spectra were generated (using AutoquantPro, MIDAC Corporation) by normalizing the measured spectra to a background spectrum (that contained the least absorption due to volcanic gases). The absorbance spectra were used to calculate concentration path lengths for the major species (H_2O, SO_2, CO_2, HCl, H_2S, HF, and CO). Analyses were performed in the window 2178–2189 cm^{-1} for H_2O and 2264–2273 cm^{-1} for CO_2. Relative errors range from 2%–3% (SO_2 and HCl) to 5.5%–7.5% (H_2O and CO_2) to 10%–12% (H_2S). The molar concentration ratios between species, derived from plots of concentration path lengths, were used to calculate gas compositions. The retrieval technique is discussed in more detail elsewhere (Edmonds and Gerlach, 2006).

Table 1 shows the mean composition of gases emitted during the three observed styles of degassing. On 9 December 2004, OP FTIR measurements were carried out during a gas piston event at the January vent in the crater of Pu`u`Ō`ō (Fig. 1B). A low rumbling from the vent from 12:01–12:19 was followed by a loud roaring from 12:20–12:27; from 12:12–12:22, incandescence from the vent became steadily brighter. During the low rumbling, the amount of SO_2 in the path length (assumed to be proportional to the flux) decreased steadily, the proportions of H_2O, SO_2, HCl, and HF decreased, the proportion of CO_2 and H_2S in the gas phase increased, and molar H_2O/CO_2 and SO_2/H_2S decreased (Figs. 2A–2D). During the loud roaring, SO_2 flux was low, the flux of CO_2 was high, the molar fractions of CO_2 and H_2S were high, the fractions of H_2O and SO_2 were low, and molar H_2O/CO_2 and SO_2/H_2S increased (Figs. 2A–2D). Between 12:20 and 12:21 two consecutive spectra yielded a gas composition with >60 mol% CO_2 and >6 mol% H_2S. The average gas CO_2 content from 12:20 to 12:22 was 31.1 mol%, and from 12:20 to 12:27, 13.7 mol% (Table 1). After 12:28, the gas returned to a composition that was more typical of persistent, continuous degassing (Figs. 2B, 2C; Table 1).

Lava spattering was prevalent at most of the crater vents between early February and mid-March 2005. OP FTIR measurements on 11 February 2005 during spattering episodes at the East Pond vent indicated cyclic variation in the composition and amount of gas emitted (Fig. 3). The flux of H_2O and SO_2 increased after spattering, reached a maximum after 5–60 s, and then decreased to low levels before the onset of the next spattering episode (Fig. 3A). During the peak in total gas flux (Fig. 3A), the gas was rich in H_2O and SO_2 and poor in CO_2, H_2S, HCl, HF, and CO (Figs. 3B, 3C; Table 1). This composition changed gradually back towards the gas composition of persistently continuous degassing as the gas flux decreased prior to the next period of spattering (Figs. 3B, 3C; Table 1).

IMPLICATIONS OF THE CHEMICAL COMPOSITION OF SLUGS AND BUBBLES

Assuming equilibrium degassing, the composition of volcanic gases at Pu`u`Ō`ō is related to the initial melt volatile content, the degree of vapor loss, the depth at which vapor segregates from the melt, the manner in which the vapor ascends to the surface, the extent of chemical modification during ascent, the addition of external vapor (e.g., meteoric water), and the degree of magma overturn and mixing in the conduit. If we assume that the only variable during the short-lived gas piston and spattering events is the extent to which the system is open or closed with respect to vapor, the vapor composition with depth can be calculated.

Initial melt concentrations of volatiles are assumed to be ~0.7 wt% CO_2 and ~0.7 wt% H_2O (Wallace and Anderson, 1998; Gerlach et al., 2002). Solubilities of CO_2 and H_2O are from VolatileCalc (Newman and Lowenstern, 2002; Fig. 4A). Three end-member degassing scenarios are developed here: the first assumes closed-system degassing from mantle depths to the surface, whereby melt and bubbles remain in equilibrium and in physical contact. The second, partially open-system degassing, assumes that all vapor bubbles are lost from the summit magma chamber (at ~3 km depth), escaping through the caldera floor at the summit of Kilauea (after Gerlach and Graeber, 1985); thereafter, bubbles nucleate and evolve in a closed system. The third case, open-system degassing, assumes that vapor is continually lost after exsolving from the melt throughout magma ascent. The CO_2 content and the molar H_2O/CO_2 of the vapor differ by orders of magnitude for each regime, making them sensitive indicators of vapor segregation processes (Figs. 4B, 4C).

Gas emitted during persistent continuous degassing has a mean CO_2 content of ~3.85 mol% and a mean H_2O/CO_2 of ~23 (Table 1). This gas composition is similar to type II gases measured by Gerlach and Graeber (1985). This gas is (1) in equilibrium with melt that has undergone partially open-system degassing at depths of <100 m (Fig. 4), or

TABLE 1. MEAN GAS COMPOSITION DURING THREE STYLES OF DEGASSING*

		Gas pistoning				Spattering	
Species	PCD	12:21	Mean (12:20–12:21)	Mean (12:21–12:27)	12:28	Mean (spatter)	Mean (between spatter)
n	7233	1	15	20	1	65	88
H_2O	89.8	18.1	61.4	80.1	81.6	92.0	81.8
SO_2	5.72	0.97	1.02	2.73	12.9	7.17	9.47
CO_2	3.85	69.1	31.1	13.6	3.80	0.346	6.44
HCl	0.249	1.72	0.916	0.575	0.500	0.263	1.08
HF	0.174	1.68	0.884	0.497	0.240	0.0371	0.451
H_2S	0.172	8.37	5.00	2.65	1.02	0.161	1.25
CO	0.027	bd	bd	bd	bd	0.0165	0.0494
C/S	0.66	70.0	30.0	5.0	0.3	0.05	0.7
H_2O/CO_2	23.0	0.3	2.0	5.9	21.0	270.0	13.0

*Mean gas composition during persistent continuous degassing (PCD) as calculated from 4200 spectra over 20 days; during a gas piston event on 9 December 2004; and during lava spattering on 11 February 2005. bd—below detection.

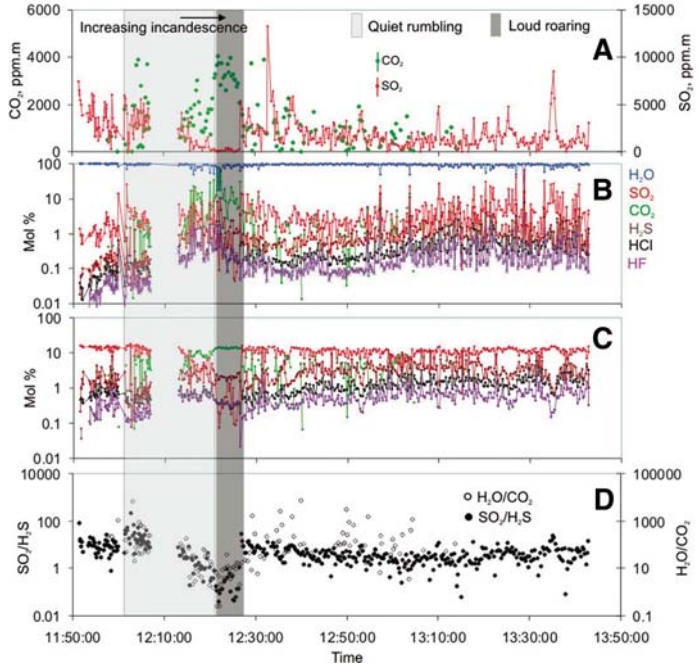

Figure 2. A: SO_2 and CO_2 concentration path length. B: Gas composition. C: Gas composition, recalculated to constant H_2O. D: Molar H_2O/CO_2 and SO_2/H_2S through time during gas piston event on 9 December 2004. Arrow shows increasing incandescence.

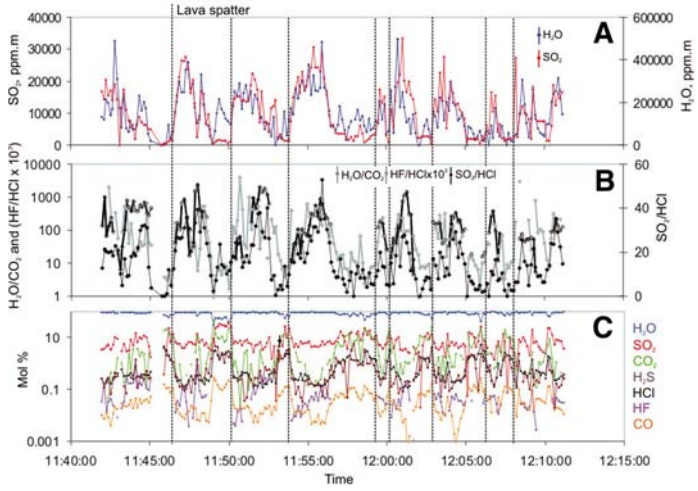

Figure 3. A: SO_2 and H_2O concentration path length. B: Molar H_2O/CO_2, HF/HCl, and SO_2/HCl. C: Gas composition through time during lava spattering on 11 February 2005.

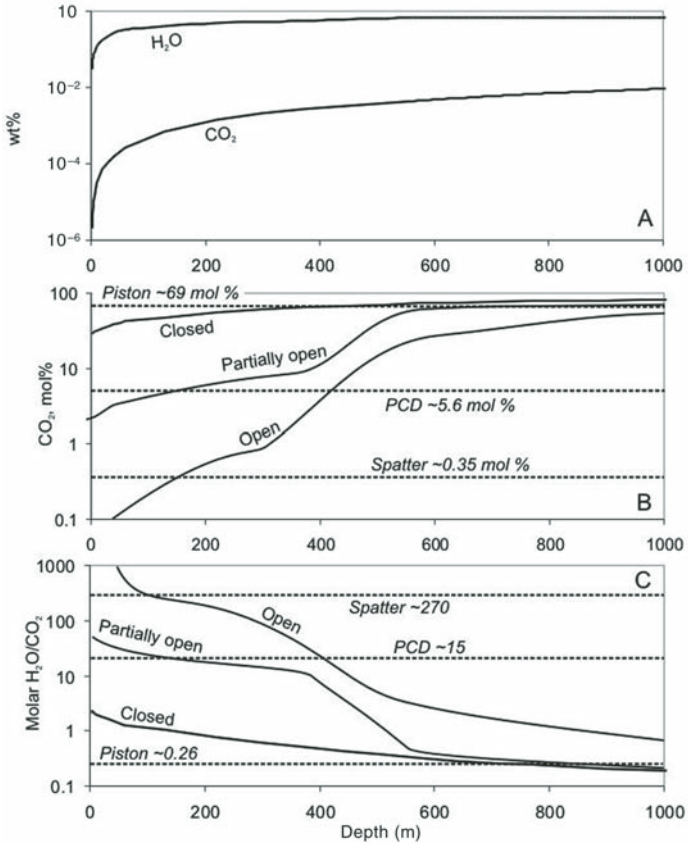

Figure 4. A: Melt H_2O and CO_2 contents with depth used for calculations. B: CO_2 mol% and molar H_2O/CO_2 (C; both solid lines) of vapor with depth for three degassing regimes (see text). Data for persistent continuous degassing (PCD), gas piston events, and lava spattering are marked with dashed lines.

(2) in equilibrium with a mixed melt at ~200–400 m depth undergoing open- and partially open-system degassing (Fig. 4), or (3) a result of the bursting of a mixture of bubbles in equilibrium with melt at atmospheric pressure: some nucleated at depth and remained in suspension in the summit magma chamber and some nucleated after leaving the summit magma chamber (mixing between the closed and partially open regimes in Fig. 4). Magma ascends, degasses as bubbles burst at the surface, and then overturns beneath the crater vents. The degassed lava then erupts effusively from the south flank vents.

The gas emitted at 12:21 on 9 December 2004 during the gas piston event contained ~69 mol% CO_2 (Table 1), which would have been in equilibrium with melt at depths of 600–900 m in the case of partially open system degassing (Fig. 4B). The molar H_2O/CO_2 of the gas was 0.26, which would be in equilibrium with melt at depths of ~600–800 m (for the cases of both closed and partially open degassing; Fig. 4C). The SO_2/H_2S ratio shows a striking departure from normal gas compositions (Fig. 2D; Table 1), which also suggests a deeper origin for the gas. For normal equilibrium degassing conditions of 1 atm, 1400 K, using an NNO-0.5 buffer, SO_2/H_2S is 50–100 for Kilauea gases (Gerlach, 2004; this work). The fraction of H_2S in the vapor increases with pressure, owing to the volume difference in the reaction $SO_2 + 3H_2 \leftrightarrow H_2S + 2H_2O$. The abundance of H_2S will be greater than SO_2 in the gas phase at lithostatic pressures greater than a few MPa, or a few hundred meters (for the redox buffer of NNO-0.5 at 1400 K) over a range of basic magma compositions and initial sulfur content (Moretti et al., 2003).

The gas piston event involved the rapid transport of a slug of gas from 600 to 900 m depth beneath Pu`u`Ō`ō to the surface. This is consistent with the location of the seismic tremor associated with gas piston events at 100–500 m beneath the surface (Goldstein and Chouet, 1994). As the gas slug ascends, it expands and fills the conduit, displacing melt upward (as proposed by Swanson et al., 1979), resulting in the rumbling sound and the increase in incandescence. The decrease in the flux of SO_2 and H_2O during this period was caused by a reduction in the volume of degassing melt in the conduit due to displacement, whereby melt drained down the conduit walls as the slug ascended. The slug moved rapidly relative to the melt; modification of its chemical composition was minimal. Seyfried and Freundt (2000) showed that single gas slugs can form in a

volcanic conduit after a sudden injection of a limited gas volume to its base; the average scaled ascent velocity of the slug was 1–3 m/s using a conduit diameter of 5 m, a magma viscosity of 500 Pa·s and density of 2600 kg/m^3. Transport of a gas slug up a 400–900 m conduit would require ~3–12 min, a range that encompasses the time scale of observed increasing incandescence (10 min; Fig. 2). A burst of CO_2- and H_2S-rich gas and a loud roaring sound accompanied the arrival of the main slug at the surface at 12:21. Smaller gas slugs may have risen at slightly lower speeds and their composition been modified by exsolution and dilution, causing the scatter in gas compositions measured from 12:22 to 12:27 (Fig. 2). The harvesting of smaller bubbles during ascent would tend to lower the CO_2 concentration; the estimated depth is therefore a minimum. The high CO_2 content of the slugs precludes significant shallow bubble harvesting as a mechanism for slug formation and instead supports the idea of accumulation of vapor at a fixed depth before transport up the conduit, in the manner suggested by Jaupart and Vergniolle (1989). These measurements do not support the notion of gas accumulation beneath a shallow, viscous, degassed cap, as proposed by Johnson et al. (2005), which would tend to lead to the accumulation of H_2O-rich instead of CO_2-rich vapor. Similarly, accumulation of deep-sourced vapor has been demonstrated to precede Strombolian events at Yasur Volcano (Oppenheimer et al., 2006) and at Etna Volcano, Italy; accumulation of CO_2-rich vapor and foam collapse was proposed to drive lava fountaining (Allard et al., 2005).

Bubbles bursting at the surface during lava spattering are richer in H_2O and poorer in CO_2 than gases emitted during persistent continuous degassing (Fig. 3; Table 1). The CO_2 content of the spatter gas is ~0.35 mol% and the molar H_2O/CO_2 is ~270 (Table 1), diagnostic of fully open-system degassing within 100–150 m of the surface (Figs. 4B, 4C). Alternatively, magma may be ascending rapidly, leading to supersaturation with respect to CO_2; if this were the case, however, bubbles would have to attain unrealistic sizes in order to rise relative to the melt. As bubbles ascend, expansion occurs due to volatile exsolution, decompression, and dynamic coalescence, causing them to grow and consequently accelerate toward the surface; a bubble 4 mm across will rise at a speed of 1 mm/s, while a 4 cm bubble will rise at 10 cm/s relative to the host melt (from Stoke's Law). Bubbles are likely to attain larger sizes if the magma is relatively stagnant in the conduit, as they have more time and opportunity for coalescence during ascent. Overpressured bubbles burst vigorously at the surface and the bubble walls (the spatter) are propelled several tens of meters above the vent. The segregation of vapor by the ascent of large bubbles at the crater vents efficiently strips the conduit magma of volatiles; the degassed lava then erupts from vents on the south flank of Pu`u`Ō`ō.

CONCLUSIONS

Gas segregated from melt ascending beneath Pu`u`Ō`ō in three contrasting ways during 2004–2005. Persistent continuous degassing from the crater vents occurs when magma ascends and suspended bubbles burst at the surface; magma overturns and degassed magma erupts from flank vents. These gases are generally H_2O rich, with a molar C/S <1. Gas piston events occur when CO_2-rich (up to 67 mol% CO_2) gas slugs, which accumulate at some fixed depth between 600 and 900 m beneath Pu`u`Ō`ō, are sporadically released and travel up the conduit at a few meters per second. Lava spattering is caused by the bursting of large, H_2O-rich bubbles (with relatively low CO_2 and SO_2) formed by dynamic coalescence during open-system degassing at depths of <150 m. This style of activity occurs when magma is relatively stagnant beneath Pu`u`Ō`ō. Convective degassing and dynamic bubble coalescence effectively strip the melt of gases and cause dominantly effusive activity during the current stage of the eruption; gas piston events involve deep, CO_2-rich gases, and thus their occurrence does not preclude fountains driven by H_2O degassing near to the surface.

ACKNOWLEDGMENTS

This research was carried out with the support of a U.S. Geological Survey Mendenhall Fellowship and the Center for the Study of Active Volcanoes at the University of Hawaii, Hilo. We thank Paul Wallace, Patrick Allard, and Thierry Menand for detailed reviews that improved the paper.

REFERENCES CITED

Allard, P., Burton, M., and Mure, F., 2005, Spectroscopic evidence for a lava fountain driven by previously accumulated magmatic gas: Nature, v. 433, p. 407–410.

Edmonds, M., and Gerlach, T.M., 2006, The airborne lava-seawater interaction plume at Kilauea Volcano, Hawaii: Earth and Planetary Science Letters, v. 244, p. 83–96.

Gerlach, T.M., 2004, Comment: Morphology and compositions of spinel in Pu′u′Ō′ō lava (1996–1998), Kilauea volcano, Hawaii'—Enigmatic discrepancies between lava and gas-based *f*O2 determinations of Pu′u′Ō′ō lava: Journal of Volcanology and Geothermal Research, v. 134, p. 241–244.

Gerlach, T.M., and Graeber, E.J., 1985, Volatile budget of Kilauea Volcano: Nature, v. 313, p. 273–277.

Gerlach, T.M., McGee, K.A., Elias, T., Sutton, A.J., and Doukas, M.P., 2002, Carbon dioxide emission rate of Kilauea Volcano: Implications for primary magma and the summit reservoir: Journal of Geophysical Research, v. 107, ECV 3–1 to ECV 3–15, doi: 10.1029/2001JB000407.

Goldstein, P., and Chouet, B., 1994, Array measurements and modeling of sources of shallow volcanic tremor at Kilauea Volcano, Hawaii: Journal of Geophysical Research, v. 99, p. 2637–2652.

Head, J.W., and Wilson, L., 1987, Lava fountain heights at Pu'u 'O'o, Kilauea, Hawaii: Indicators of amount and variations of exsolved magma volatiles: Journal of Geophysical Research, v. 92, p. 13,715–13,719.

Herd, R.A., and Pinkerton, H., 1997, Bubble coalescence in basaltic lava: Its impact on the evolution of bubble populations: Journal of Volcanology and Geothermal Research, v. 75, p. 137–157.

Jaupart, C., and Tait, S., 1990, Dynamics of eruptive phenomena, *in* Nicholls, J., and Russell, J.K., eds., Modern methods of igneous petrology: Understanding magmatic processes: Mineralogical Society of America Reviews in Mineralogy, v. 24, p. 213–238.

Jaupart, C., and Vergniolle, S., 1989, The generation and collapse of a foam layer at the roof of a basaltic magma chamber: Journal of Fluid Mechanics, v. 203, p. 347–380.

Johnson, J.B., Harris, A.J.L., and Hoblitt, R.P., 2005, Thermal observations of gas pistoning at Kilauea Volcano: Journal of Geophysical Research, v. 110, doi: 10.1029/2005JB003944.

Moretti, R., Papale, P., and Ottonello, G., 2003, A model for the saturation of C-O-H-S fluids in silicate melts: Geological Society [London] Special Publication 213, p. 81–102.

Newman, S., and Lowenstern, J.B., 2002, VolatileCalc; a silicate melt-H_2O-CO_2 solution model written in Visual Basic for Excel: Computers & Geosciences, v. 28, p. 597–604.

Oppenheimer, C., Bani, P., Calkins, J.A., Burton, M.R., and Sawyer, G.M., 2006, Rapid FTIR sensing of volcanic gases released by Strombolian explosions at Yasur volcano, Vanuatu: Applied Physics B: Lasers and Optics, v. 85, p. 453-460, doi: 10.1007/s00340–006–2353–4.

Ryan, M.P., Koyanagi, R.Y., and Fiske, R.S., 1981, Modeling the three-dimensional structure of macroscopic magma transport systems: Application to Kilauea Volcano, Hawaii: Journal of Geophysical Research, v. 86, p. 7111–7129.

Seyfried, R., and Freundt, A., 2000, Experiments on conduit flow and eruption behaviour of basaltic eruptions: Journal of Geophysical Research, v. 105, p. 23,727–23,740.

Swanson, D.A., Duffield, W.A., Jackson, D.B., and Peterson, D.W., 1979, Chronological narrative of the 1969–71 Mauna Ulu eruption of Kilauea Volcano, Hawaii: U.S. Geological Survey Professional Paper 1056, 55 p.

Tazieff, H., 1994, Permanent lava lakes: Observed facts and induced mechanisms: Journal of Volcanology and Geothermal Research, v. 63, p. 3–11.

Wallace, P.J., and Anderson, A.T., Jr., 1998, Effects of eruption and lava drainback on the H_2O contents of basaltic magmas at Kilauea Volcano: Bulletin of Volcanology, v. 59, p. 327–344.

Manuscript received 18 October 2006
Revised manuscript received 1 March 2007
Manuscript accepted 23 March 2007

Printed in USA